nature structural & molecular biology

Structural and biochemical insights into the regulation of protein phosphatase 2A by small t antigen of SV40

Yu Chen[1,2], Yanhui Xu[1,2], Qing Bao[1], Yongna Xing[1], Zhu Li[1], Zheng Lin[1], Jeffry B Stock[1], Philip D Jeffrey[1] & Yigong Shi[1]

The small t antigen (ST) of DNA tumor virus SV40 facilitates cellular transformation by disrupting the functions of protein phosphatase 2A (PP2A) through a poorly defined mechanism. The crystal structure of the core domain of SV40 ST bound to the scaffolding subunit of human PP2A reveals that the ST core domain has a novel zinc-binding fold and interacts with the conserved ridge of HEAT repeats 3–6, which overlaps with the binding site for the B′ (also called PR61 or B56) regulatory subunit. ST has a lower binding affinity than B′ for the PP2A core enzyme. Consequently, ST does not efficiently displace B′ from PP2A holoenzymes *in vitro*. Notably, ST inhibits PP2A phosphatase activity through its N-terminal J domain. These findings suggest that ST may function mainly by inhibiting the phosphatase activity of the PP2A core enzyme, and to a lesser extent by modulating assembly of the PP2A holoenzymes.

PP2A is a major protein serine/threonine phosphatase and is involved in many essential aspects of cellular physiology[1–3]. PP2A exists in two major forms in cells: the heterodimeric core enzyme and the heterotrimeric holoenzyme[4]. The PP2A core enzyme consists of a catalytic subunit, or C subunit, and a scaffolding subunit, known as the A or PR65 subunit. To gain full activity toward specific substrates and for appropriate cellular localization, the PP2A core enzyme interacts with a variable regulatory subunit to form a heterotrimeric holoenzyme. In mammalian cells, the A and C subunits each have two isoforms, which share high sequence similarity[5–8]. There are at least 16 regulatory subunits, belonging to four subfamilies[1,3,9]: B (also called B55 or PR55), B′ (also called B56 or PR61), B″ (also called PR72) and B‴ (also called Striatin, PR93 or PR110).

The virus-encoded tumor antigens of DNA tumor viruses SV40 and polyomavirus are essential in cellular transformation[10]. In SV40, the large T antigen (LT) inactivates p53 and Rb, two tumor-suppressor proteins, whereas ST targets PP2A[10,11]. PP2A is the only protein known to interact with ST in cells[12,13]. Interaction of PP2A with ST results in stimulation of the MAP kinase pathway and induction of cell proliferation[14]. Notably, ST seems to be required for SV40-mediated cellular transformation and tumor formation[15]. These observations underscore the significance of the interaction between ST and PP2A.

ST of SV40 directly interacts with the A subunit of PP2A. The results of mutagenesis of the A subunit have identified HEAT repeats 3–6 as the primary binding element for ST[16,17]. A single missense mutation, R183E/A or M180A, in the fifth HEAT repeat of the A subunit markedly compromises binding to ST[18]. Deletion analysis has identified the C-terminal fragment of ST as necessary and sufficient for binding to the A subunit of PP2A[19].

How does ST interfere with the normal functions of PP2A? Early experimental evidence favored a model in which ST binding results in alteration of the phosphatase activity of PP2A[20–23]. More recent studies seem to suggest that ST may function by displacing the regulatory subunits from the PP2A holoenzymes, hence antagonizing the normal functions of PP2A[11,24]. Supporting the latter model is the finding that ST forms a stable complex only with the PP2A core enzyme and not with the holoenzyme[12,13]. Subsequent investigations have suggested that ST might displace the B subunits from the PP2A holoenzyme[14,21,25]. Still more recently, suppression of the γ isoform of B′ (B′γ) expression has been shown to inhibit PP2A activity, lowering it to a level similar to that achieved by overexpression of ST[26]. This observation was taken to imply that ST might displace the B′γ subunit from the holoenzyme.

Despite these biochemical characterizations, how ST interferes with the normal functions of PP2A remains enigmatic, in part owing to a lack of quantitative and structural information. For example, the binding affinity between the PP2A core enzyme and ST has yet to be determined, and it is unclear whether ST binds the PP2A core enzyme with a higher affinity than those of the regulatory subunits. In addition, displacement of a regulatory subunit from the PP2A holoenzyme by ST has yet to be demonstrated *in vitro* using purified recombinant proteins. Last but not least, it is not yet understood how ST specifically recognizes PP2A. Answers to these questions are expected to reveal insights into the regulation of PP2A function by ST.

[1]Department of Molecular Biology, Lewis Thomas Laboratory, Princeton University, Princeton, New Jersey 08544, USA. [2]These authors contributed equally to this work. Correspondence should be addressed to Y.S. (ygshi@princeton.edu).

Received 25 March; accepted 25 April; published online 27 May 2007; doi:10.1038/nsmb1254

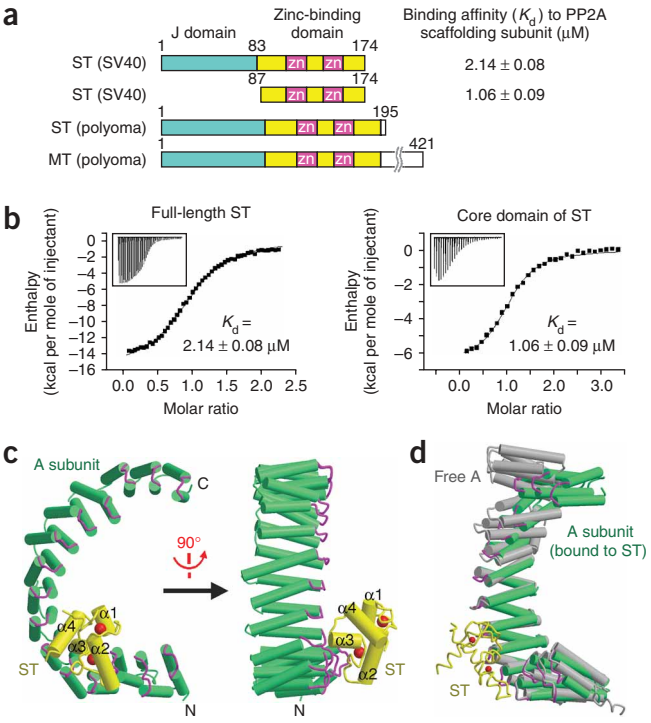

Figure 1 Structure of the scaffolding subunit of PP2A bound to SV40 ST. (**a**) A core domain in ST is responsible for binding PP2A. There are two conserved domains in ST of SV40 and ST and MT of polyomavirus: an N-terminal J domain and a C-terminal zinc-binding domain. Limited proteolysis identified the zinc-binding domain as a stable structural core. This core domain is necessary and sufficient for binding to the A subunit of PP2A. (**b**) ITC measurements showing that the core domain of ST binds the A subunit of PP2A approximately two-fold more tightly than does full-length ST. Insets, titration traces. K_d ± s.d. is shown. (**c**) Overall structure of A subunit of PP2A (green) bound to core domain of SV40 ST (yellow). Conserved ridge of A subunit is colored magenta. The two zinc atoms are in red. All structural figures were prepared using MOLSCRIPT[46]. (**d**) Comparison of structures of A subunit unbound (gray) or bound (green) to ST, showing conformational variation in the C-terminal HEAT repeats. Because no protein is bound to the HEAT repeats, this probably reflects the inherent conformational flexibility of the A subunit.

To elucidate the mechanisms by which ST inhibits the normal functions of PP2A, we have determined the crystal structure of the core domain of ST bound to the A subunit of PP2A and performed associated biochemical analyses. Our results suggest that ST functions as a switch to alter the phosphatase activity of PP2A. It does so in two ways: by inhibiting the phosphatase activity of the PP2A core enzyme through direct binding and, to a lesser extent, by modulating assembly of the PP2A holoenzyme.

RESULTS

Characterization of ST binding to PP2A

Previous studies have shown that ST forms a stable complex with the free A subunit or the PP2A core enzyme, but not with the C subunit, indicating that the primary interactions between PP2A and ST occur through the A subunit[21]. Full-length ST (residues 1–174) from SV40 was overexpressed in *Escherichia coli* and purified to homogeneity. As previously reported, ST formed a stable complex with the A subunit of PP2A (data not shown).

The N-terminal domain (residues 1–83) of ST shares sequence homology with the J domain of DnaJ from *E. coli* (**Fig. 1a**). The C-terminal region of ST is thought to coordinate two zinc atoms and is responsible for interaction with the A subunit of PP2A[19] (**Fig. 1a**). To identify the structural core domain required for binding to PP2A, we subjected full-length ST to limited proteolysis. This analysis identified a 9-kDa core domain (residues 87–174) that is resistant to cleavage by elastase. Using isothermal titration calorimetry (ITC), we determined the K_d for binding between full-length ST and the A subunit of PP2A to be approximately 2.14 ± 0.08 μM (**Fig. 1b**). In contrast, the K_d for binding between the core domain of ST and the A subunit was approximately 1.06 ± 0.09 μM (**Fig. 1b**). This analysis shows that, compared with full-length ST, the core domain retains a full-strength interaction with the A subunit of PP2A.

Structure of the A–ST complex

We crystallized the core domain of ST (residues 87–174) bound to the α isoform of the A subunit of PP2A. The crystals belong to the space group $C222_1$ and contain two complexes per asymmetric unit. The structure was determined at 3.3-Å resolution by molecular replacement (**Fig. 1c**). The two PP2A A–ST complexes can be superimposed with an r.m.s. deviation of 1.77 Å over 521 aligned α carbon atoms, and the structural features we wish to discuss are identical between them. For simplicity, we limit our discussion to one such complex between ST and the A subunit of PP2A.

The core domain of ST comprises four α-helices (α1–α4) and has a compact, globular fold (**Fig. 1c**). The core domain of ST interacts with the conserved ridge of HEAT repeats 3–6 in the A subunit of PP2A (**Fig. 1c**). Compared with the free A subunit, binding by ST does not induce appreciable conformational changes in HEAT repeats 1–10. Notably, although HEAT repeats 11–15 are not involved in binding ST, they have a different conformation from that of the free A subunit (**Fig. 1d**). This structural difference is apparently a result of crystal packing interactions and probably reflects the inherently flexible nature of the HEAT repeats in the A subunit of PP2A, as previously observed[27–30].

Structural features of ST

The four α-helices in the core domain of ST are organized around two zinc atoms, confirming an earlier prediction[31]. These two zinc atoms are important in the structure and stabilize the overall fold of ST. In contrast to the prediction that ST may contain a GAL4-like Zn_2-Cys_6 binuclear cluster[31], the two zinc atoms are coordinated by seven cysteine residues and one histidine residue, all located in the first three helices and the intervening loops (**Fig. 2a**). The first zinc atom is chelated by four cysteine residues, Cys103, Cys111, Cys113 and Cys116, whereas the second zinc atom is coordinated by one histidine and three cysteine residues: His122, Cys138, Cys140 and Cys143. All zinc-binding residues are conserved in ST and middle T antigen (MT) of polyomavirus (**Fig. 2a**). Notably, these two zinc-binding sites are structurally similar in the region encompassing the second, third and fourth zinc-coordinating cysteine residues, with an r.m.s. deviation of 0.56 Å over 13 aligned α carbon atoms (**Fig. 2b**).

To gain functional insights, we searched for structural homologs of the ST core domain using Dali[32]. The search did not identify any protein with noticeable homology. There were only six structures with *Z*-scores (similarity score) greater than 2.0, and the closest hit (PDB 1XKG) had a *Z*-score of 2.8 and an r.m.s. deviation of 2.3 Å over 34 α carbon atoms. Closer examination in O[33] revealed that these six structures are dissimilar to that of the core domain of ST. We concluded that the structure of the ST core domain probably represents a novel zinc-binding fold.

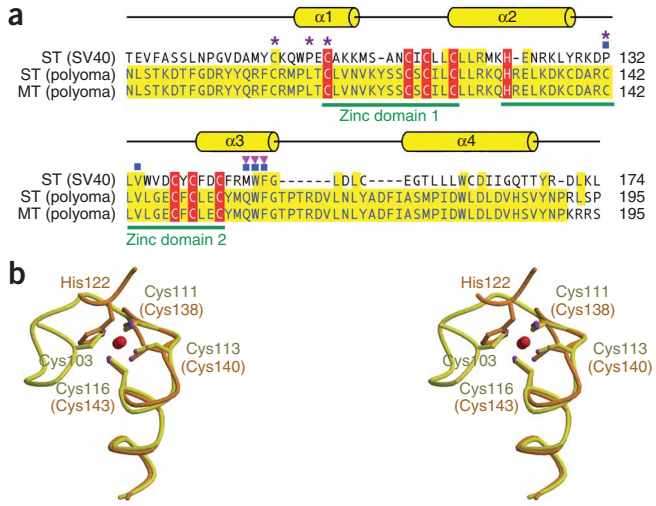

Figure 2 Structural features of the core domain of ST. (**a**) Sequence alignment of ST from SV40 and ST and MT from polyomavirus. Yellow, conserved residues; red, zinc-binding residues; blue squares and magenta triangles, residues that interact with the A subunit of PP2A through hydrogen bonds and van der Waals contacts, respectively; purple asterisks, residues whose mutation abrogates interaction with the A subunit[18,35]. (**b**) Superposition showing structural similarity between zinc-binding motifs 1 and 2 in ST (colored yellow and orange, respectively).

Recognition of PP2A by ST

Residues from helix α3 and the preceding loop between α2 and α3 of ST recognize the conserved ridge of HEAT repeats 3–6 in the A subunit of PP2A (**Fig. 3a**), through both hydrogen bonds and van der Waals interactions. These interactions result in the burial of 1,050 Å^2 of exposed surface area.

Five hydrophobic residues in ST and seven residues in the A subunit form a network of van der Waals interactions at the interface (**Fig. 3b,c**). Pro132 and Val134, both located in the loop between α2 and α3 of ST, stack against the side chains of Glu100 (HEAT3), Trp140 (HEAT4), Phe141 (HEAT4) and Thr178 (HEAT5) (**Fig. 3b**). Met146, Trp147 and Phe148, all located in helix α3 in the core domain of ST, make van der Waals contacts to Phe141 (HEAT4), Pro179 (HEAT5), Met180 (HEAT5), and Gln217 (HEAT6). These interactions are buttressed by three intermolecular hydrogen bonds. Arg183 in the A subunit donates a pair of hydrogen bonds to the backbone carbonyl oxygen atoms of Met146 and Trp147 in ST, whereas Ser219 makes a contact to the carbonyl oxygen atom of Phe148 in ST (**Fig. 3b,c**).

The residues in SV40 ST that mediate interactions with the A subunit of PP2A are highly conserved in the ST and MT of polyomavirus (**Fig. 2b**). Of the five residues in SV40 ST that interact with PP2A, Val134, Trp147 and Phe148 are invariant, and Pro132 and Met146 are replaced by residues that can fulfill the same function at the interface. Conversely, the residues in the α isoform of the A subunit (Aα) that mediate interactions with ST are also conserved in Aβ (**Fig. 3c**). This analysis indicates that the interactions between SV40 ST and the A subunit are most probably conserved in complexes between ST or MT of polyomavirus and the A subunit.

Structural basis for published biochemical data

The structural observations provide a molecular rationale for a body of published biochemical and mutagenesis results on the interaction between SV40 ST and PP2A[16–19,34]. For example, a single missense mutation in the A subunit, such as M180A, R183A or R183E, leads to complete abrogation of interaction with ST[18]. As described above, Met180 and Arg183 are important in the interface (**Fig. 3b,c**); mutation of these residues should destabilize the interface. Another loss-of-interaction mutation is Asp139-Trp140-Phe141→His139-Ala140-Ala141 in the A subunit[18]; two of the three residues, Trp140 and Phe141, stabilize the interface through van der Waals interactions (**Fig. 3b,c**). In addition, the mutation C103S in ST results in loss of interaction with the A subunit[34]; Cys103 contributes to the structural stability of ST by coordinating a zinc ion (**Fig. 2b**).

The structural observations also nicely explain the mutagenesis data on the interactions between PP2A and ST or MT of polyomavirus[35]. The missense mutation C142Y in ST or MT of polyomavirus results in abrogation of interaction with PP2A[35]. Cys142 in ST and MT of polyomavirus corresponds to Pro132 in ST of SV40 (**Fig. 2a**), which makes van der Waals contacts to the side chains of Glu100, Trp140 and Phe141 in the A subunit (**Fig. 3b**). Analysis of the interface indicates that mutation of Cys142 to the much bulkier residue tyrosine would lead to serious steric clash with the surrounding residues in the A subunit. Another loss-of-interaction mutation in ST or MT of polyomavirus is insertion of four amino acid residues, Ala-Leu-Glu-Gln, after residue 144 (ref. 35). This insertion is located in the center of the interface between ST and the A subunit and is predicted to disrupt the interface. The mutation C111S in ST or MT of polyomavirus leads to loss of interaction with the A subunit[35]; Cys111 in ST and MT of polyomavirus corresponds to Cys103 in SV40 ST, which coordinates a zinc ion (**Fig. 2b**).

J domain contributes to binding of PP2A core enzyme

ST has previously been reported to inhibit the serine/threonine phosphatase activity of the PP2A core enzyme[20,21]. To gain insights into how ST accomplishes this task, we built an atomic model in which the core domain of ST is bound to the PP2A core enzyme (**Fig. 4a**).

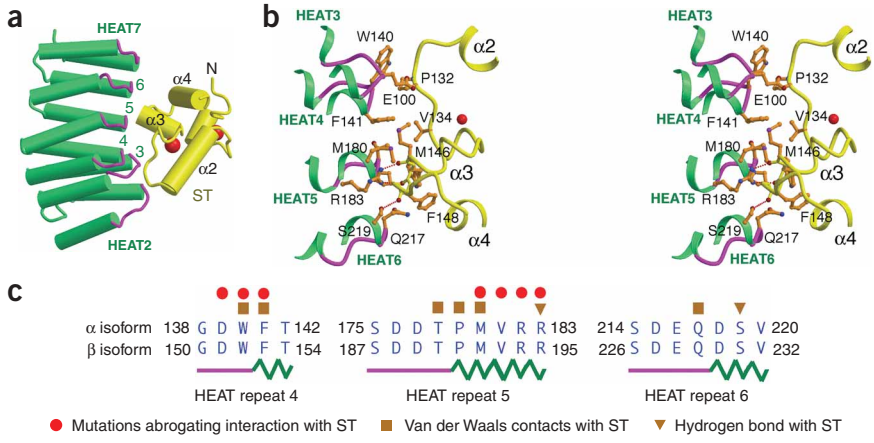

Figure 3 Recognition of the A subunit of PP2A by ST. (**a**) Close-up view of core domain of ST bound to HEAT repeats 3–6 of the A subunit of PP2A, colored as in **Figure 1**. (**b**) Stereo view of ST-A interactions. Orange sticks, side chains; red dotted lines, hydrogen bonds. (**c**) Almost all the interface residues in the A subunit of PP2A map to the conserved ridge region of HEAT repeats 4–6.

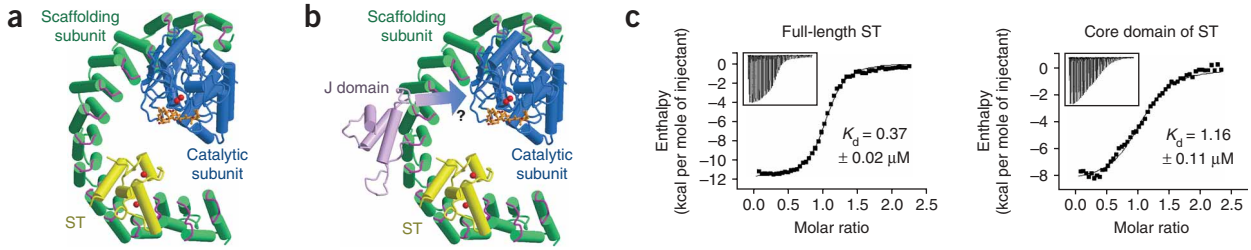

Figure 4 The J domain of ST directly contributes to binding of the PP2A core enzyme. (**a**) Atomic model of the PP2A core enzyme bound to the core domain of ST, based on two overlapping structures: the A subunit bound to ST (this study) and PP2A core enzyme (PDB 2IE3)[27]. (**b**) Model of the PP2A core enzyme bound to full-length ST. The N-terminal J domain of ST was modeled on the basis of sequence homology between ST and LT of SV40 and the available structure of the J domain of LT (PDB 1GH6)[36]. The position and the size of the J domain of ST probably allow it to directly interact with the C subunit of PP2A. (**c**) ITC measurements show that full-length ST binds the PP2A core enzyme approximately three-fold more tightly than does ST. Insets, titration traces. K_d ± s.d. is shown. This result, together with **Figure 1b**, suggests that the J domain may directly interact with the C subunit.

This model is likely to be accurate, because the binding site for ST in the A subunit in our model does not overlap with that for the C subunit in the known structure of the PP2A core enzyme (PDB 2IE3)[27]. Notably, in this model, the core domain of ST does not appear to form any direct interaction with the C subunit (**Fig. 4a**). Thus, inhibition of the PP2A serine/threonine phosphatase activity by ST probably derives from sequences other than the core domain. In particular, the N-terminal J domain of ST, which is a known protein-protein interaction motif[36], represents an ideal candidate for mediating such a function (**Fig. 4b**).

We speculated that the J domain of ST might mediate direct interaction with the C subunit of PP2A, leading to inhibition of its serine/threonine phosphatase activity (**Fig. 4b**). This hypothesis predicts that, because of the additional interactions between the J domain of ST and the C subunit of PP2A, full-length ST should bind the PP2A core enzyme with a higher binding affinity than does the core domain of ST. To test this, we measured the relevant binding affinities using ITC. Indeed, full-length ST binds the PP2A core enzyme with a K_d of 0.37 ± 0.02 μM—an approximately three-fold higher affinity than that of the core domain of ST (K_d = 1.16 ± 0.11 μM) (**Fig. 4c**).

The notion that the J domain of ST directly contributes to binding of the PP2A core enzyme is further supported by comparison of the binding affinities between ST and the PP2A core enzyme or the A subunit. On one hand, the core domain of ST has nearly identical binding affinities for the PP2A core enzyme and for the A subunit alone (**Fig. 1b** and **Fig. 4c**, right charts), indicating that the core domain of ST does not appreciably interact with the C subunit. On the other hand, full-length ST binds the PP2A core enzyme 5.78-fold more tightly than the A subunit alone (**Fig. 1b** and **Fig. 4c**, left charts). The higher binding affinity for the PP2A core enzyme is not attributable to conformational changes of the A subunit induced by the presence of the C subunit[27], because such changes are restricted to HEAT repeats 11–15, away from where ST binds.

ST inhibits the phosphatase activity of PP2A

The conclusion that the J domain of ST directly contributes to binding of the PP2A core enzyme prompted us to examine the regulation of PP2A phosphatase activity by ST. First, we reconstituted two *in vitro* phosphoserine-phosphothreonine (pSer-pThr) phosphatase assays for the PP2A core enzyme, using phosphorylase a (**Fig. 5a**) and a pThr peptide (**Fig. 5b**) as substrates. As previously reported, full-length ST inhibited the phosphatase activity of the PP2A core enzyme in a

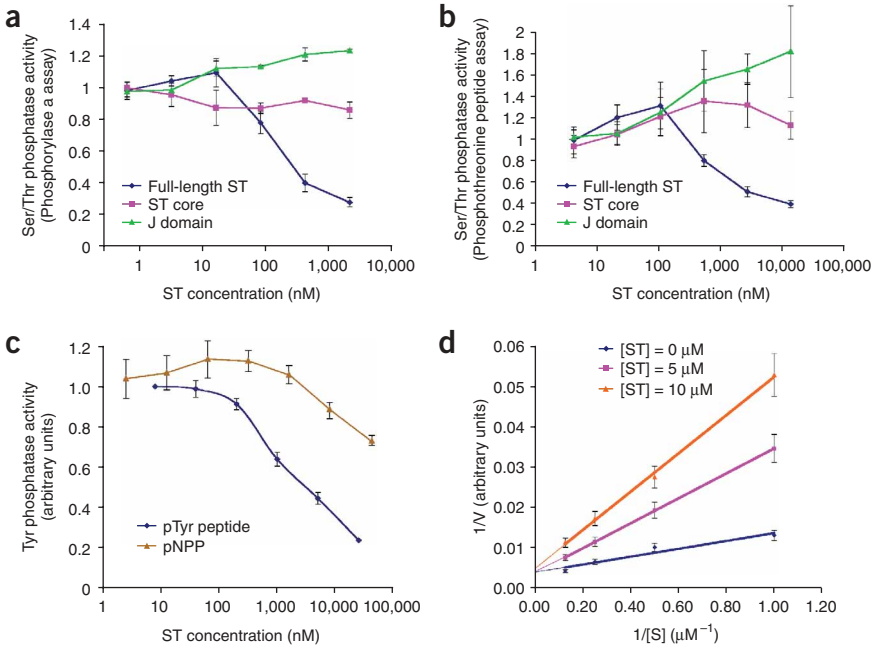

Figure 5 ST inhibits the phosphatase activity of the PP2A core enzyme. (**a**) Full-length ST, but not the core domain or the J domain, inhibits the pSer-pThr phosphatase activity of the PP2A core enzyme in a concentration-dependent manner. Phosphorylase a, which contains a pSer residue, was used as the substrate. IC_{50} for the inhibition is ~0.2 μM, consistent with the binding affinity of ST for the PP2A core enzyme. (**b**) Phosphatase assays as in **a**, using pThr peptide as the substrate. IC_{50} for the inhibition is ~2 μM. (**c**) ST inhibits the pTyr phosphatase activity of the PP2A core enzyme toward a pTyr peptide substrate, but not toward pNPP, a pTyr analog. (**d**) ST competitively inhibits the PP2A core enzyme. *V*, initial rate of pTyr phosphatase activity; [S], substrate concentration. Shown are Lineweaver-Burk plots of 1/*V* versus 1/[S], suggesting competitive inhibition in a Michaelis-Menten enzyme reaction. All error bars in **a**–**d** show s.d.

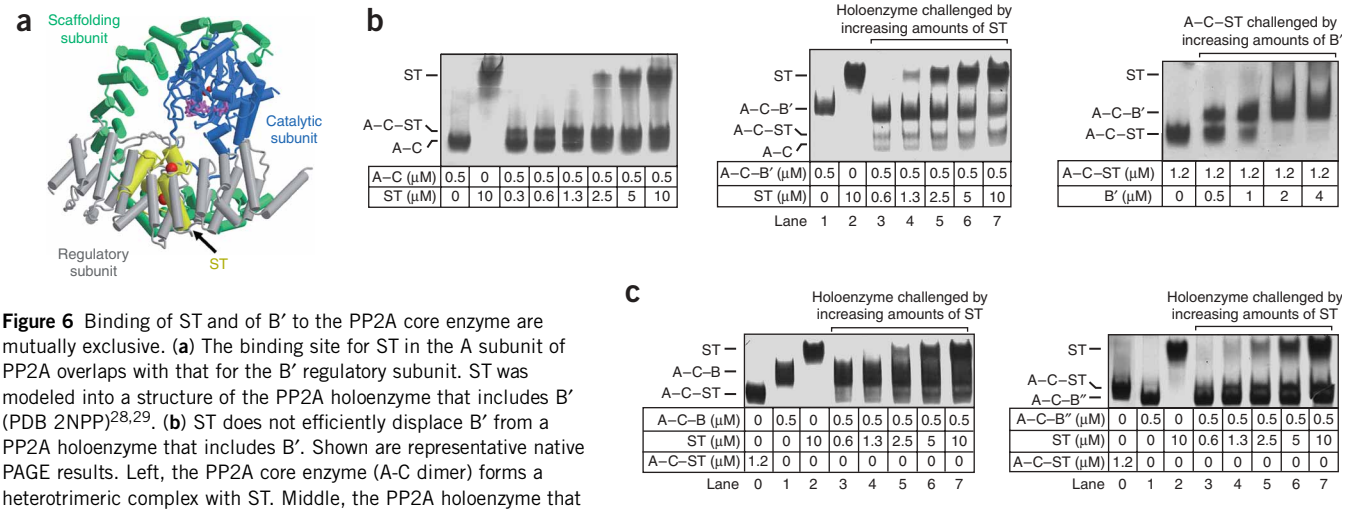

Figure 6 Binding of ST and of B′ to the PP2A core enzyme are mutually exclusive. (**a**) The binding site for ST in the A subunit of PP2A overlaps with that for the B′ regulatory subunit. ST was modeled into a structure of the PP2A holoenzyme that includes B′ (PDB 2NPP)[28,29]. (**b**) ST does not efficiently displace B′ from a PP2A holoenzyme that includes B′. Shown are representative native PAGE results. Left, the PP2A core enzyme (A-C dimer) forms a heterotrimeric complex with ST. Middle, the PP2A holoenzyme that includes the B′ subunit can withstand an excess of ST: for example, in lane 5, the concentration of ST was five-fold higher than that of the PP2A holoenzyme, yet only a small fraction of the B′ subunit was displaced. Right, the B′ subunit efficiently disrupts the A–C–ST complex in a concentration-dependent manner. (**c**) ST does not efficiently disrupt PP2A holoenzymes that include the B (left) and B″ (right) subunits. Shown are representative nondenaturing PAGE results.

concentration-dependent manner in both assays (**Fig. 5a**,**b**). The inhibition required both the core domain (residues 87–174) and the J domain (residues 1–83) of ST, because neither domain alone inhibited the PP2A core enzyme (**Fig. 5a**,**b**). Notably, the concentration of full-length ST for half-maximal inhibition of PP2A (IC_{50}) was approximately 0.2 μM in the phosphorylase a assay (**Fig. 5a**) and 2 μM in the pThr peptide assay. One obvious difference between these two assays is the size of the substrates: phosphorylase a is a phosphoprotein and is bulkier than the pThr peptide. We speculated that full-length ST does not completely block the active site of the C subunit but restricts its access, so that smaller substrates have an advantage over larger ones.

The notion of restricted access to the active site of the C subunit is supported by an additional assay, in which *p*-nitrophenylphosphate (pNPP) was used as a substrate for PP2A[37,38]. Even at high micromolar concentrations, full-length ST only slightly inhibited the phosphatase activity of PP2A toward pNPP (**Fig. 5c**). Because pNPP mimics a phosphotyrosine (pTyr) substrate, we also reconstituted a pTyr phosphatase assay using a pTyr peptide substrate as previously described[27]. In contrast to the pNPP assay, full-length ST inhibited the pTyr phosphatase activity of the PP2A core enzyme with an IC_{50} of approximately 2 μM (**Fig. 5c**), similar to that for the pThr peptide (**Fig. 5b**).

Next, we investigated the mechanism by which ST inhibits the phosphatase activity of PP2A. Two different concentrations of full-length ST, 5 and 10 μM, were used. In pilot experiments, we determined the approximate K_m values for the reactions; we used substrate concentrations around these K_m values to facilitate the analysis. We determined the initial rates (V) of the pTyr phosphatase activity of PP2A core enzyme at four substrate concentrations ([S]) in the absence or presence (5 and 10 μM) of ST. We then plotted the inverse values of initial rate ($1/V$) and substrate concentration ($1/[S]$) for each data point to obtain the Lineweaver-Burk plot (**Fig. 5d**). Analysis of the plot revealed that the data points in the absence or presence of ST could be fitted with a straight line. The extensions of these three straight lines intercept the $1/V$ axis at approximately the same point (**Fig. 5d**), a property that is indicative of competitive inhibition in a Michaelis-Menten enzyme reaction. This finding suggests that ST may inhibit the phosphatase activity of the PP2A core enzyme by competing with substrate for access to the active site. From the Lineweaver-Burk plot, we derived K_m values of 2.4 μM for the pTyr peptide in the absence of ST and 7.7 μM in the presence of 5 μM ST.

Mutually exclusive binding of ST and B′ subunit

Previous structural investigations have revealed that the B′ regulatory subunit binds the conserved ridge of HEAT repeats 2–6 in the A subunit[28,29]. Thus, the binding sites of B′ and of ST exactly overlap in the A subunit (**Fig. 6a**). The buried surface area at the A-B′ interface is 1,997 Å^2, which is approximately twice that of the A-ST interface. In addition, the B′ subunit makes noticeably more interactions with the C subunit[28,29]. This analysis suggests that formation of a PP2A holoenzyme involving the B′ subunit may exclude binding by ST. Supporting this notion, the B′ regulatory subunit interacts with the PP2A core enzyme with a K_d of approximately 0.05 μM (ref. 28), corresponding to seven-fold tighter binding than that of full-length ST.

We further investigated these binding interactions using a nondenaturing PAGE assay (**Fig. 6b**). First, we demonstrated that full-length ST formed a stable complex with the PP2A core enzyme (**Fig. 6b**, upper gel). The ternary complex between the PP2A core enzyme and ST migrated just behind the free PP2A core enzyme. Next, we titrated increasing amounts of ST into a preassembled PP2A holoenzyme involving splicing variant 1 of B′γ (B′γ1) (**Fig. 6b**, middle gel). At an approximately 1:1 molar ratio of ST to holoenzyme, only a very small fraction of the PP2A holoenzyme was converted to a ternary complex between the PP2A core enzyme and ST (**Fig. 6b**, middle gel, lane 3), indicating that ST does not efficiently compete with B′γ1 for binding to the PP2A core enzyme. Even at a ten-fold molar excess over the PP2A holoenzyme, ST did not dislodge the majority of the B′γ1 subunit from the PP2A holoenzyme (**Fig. 6b**, middle gel, lane 6). These experiments were done under conditions in which there was no free B′γ1 subunit at the beginning of incubation. In cells, the presence of free B′ subunits, albeit at low concentrations, is likely to further limit the ability of ST to displace B′ from PP2A holoenzymes. To confirm this result, we also used increasing amounts of B′γ1 to challenge the preassembled A–C–ST complex (**Fig. 6b**, bottom gel). At an approximately 1:1 molar ratio, B′γ1 displaced the vast majority of ST from the A–C–ST complex.

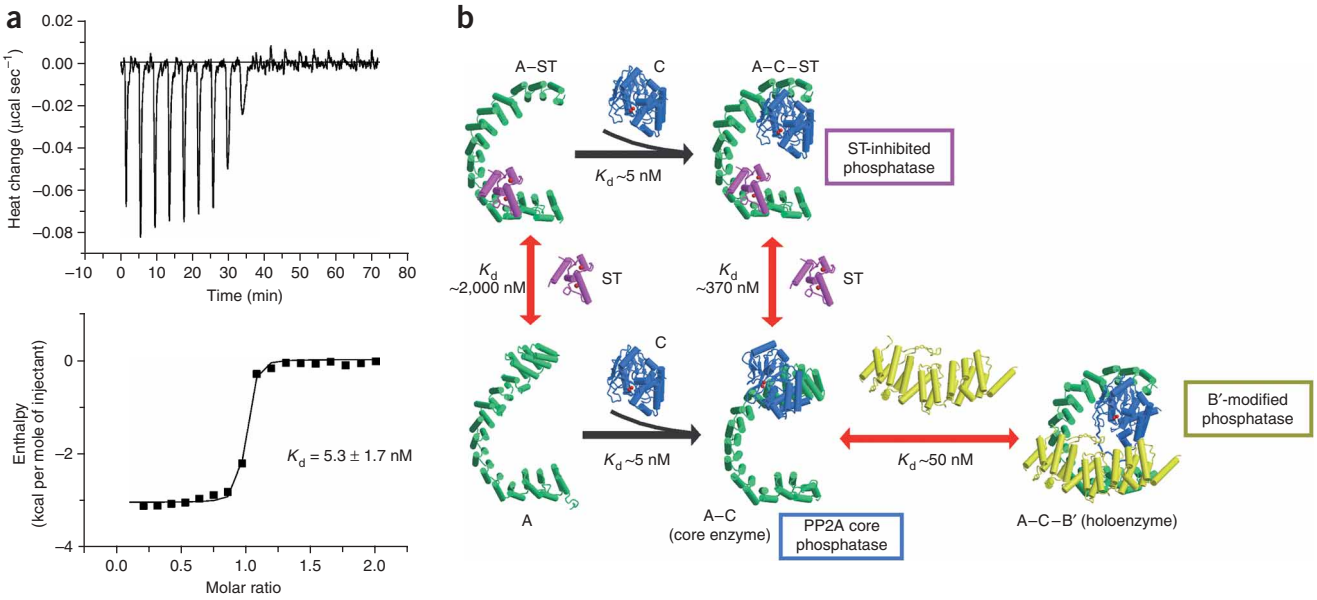

Figure 7 A proposed mechanistic model of ST-mediated inhibition of PP2A. (**a**) The C subunit binds the A subunit with a dissociation constant of ~5 nM, as determined by ITC. K_d ± s.d. is shown. (**b**) Schematic diagram illustrating the mechanisms of ST-mediated inhibition of PP2A, based on structural and biochemical information. All binding affinities shown were determined using ITC. In the absence of ST, there are two populations of PP2A: the core enzyme and the holoenzymes involving various regulatory subunits, each with a distinct substrate specificity and phosphatase activity. ST disturbs the equilibrium by forming a heterotrimeric complex with the PP2A core enzyme. This PP2A–ST complex has a different phosphatase activity and substrate specificity from the PP2A core enzyme or holoenzyme. Although the structure of ST shown is that of the core domain, the binding affinities are those of full-length ST.

Our observations strongly suggest that, unless present at a much higher concentration than the B′ regulatory subunit, ST is unlikely to displace a substantial portion of B′ from PP2A holoenzymes. This conclusion may not be incompatible with the observation that suppression of B′γ expression results in inhibition of PP2A activity to a similar level as that achieved by overexpression of ST[26]. One way to explain this observation is that the changes in PP2A activity owing to suppression of B′γ expression are similar to those achieved by overexpression of ST.

Given the contrast of our *in vitro* results with those implied by cell-based studies on B′, we also investigated whether ST could efficiently displace the B and B″ subunits from preassembled PP2A holoenzymes, using nondenaturing gel-shift assays (**Fig. 6c**). To our surprise, although ST was able to displace B (top gel) or B″ (bottom gel) from their respective holoenzymes, the displacement was inefficient and required a marked excess of ST. One important caveat is that these observations are entirely based on *in vitro* experiments using purified recombinant proteins. The circumstances could be different in cells. For example, the J domain of ST has been shown to stimulate the ATPase activity of Hsc70 by four- to nine-fold[39], and it has been hypothesized that this activity could be harnessed to disassemble multiprotein complexes *in vivo*[39]. Thus, ST might be able to cooperate with cellular factors to disassemble PP2A holoenzymes in cells[39]. Such a hypothesis might explain a large body of contrasting observations, both *in vivo* and *in vitro*.

DISCUSSION

In this study, we report quantitative measurements of binding affinities between ST and PP2A. To our surprise, ST binds the PP2A core enzyme with a lower affinity than does the B′ subunit. Supporting this observation, ST did not efficiently displace B′ from PP2A holoenzymes, whereas B′ readily disrupted a preassembled complex between ST and the PP2A core enzyme. These *in vitro* results have important implications for the interpretation of experimental observations derived from cell-based studies. So that we could propose a meaningful model of PP2A regulation, we also measured the binding affinity between the A and C subunits using ITC (**Fig. 7a**). The affinity (5.3 ± 1.7 nM) is considerably lower than that estimated by another study, in which the inhibition IC_{50} of myosin light-chain phosphatase activity of the C subunit by the A subunit was taken to be the dissociation constant[40]. This discrepancy is probably due to the different methods used. Nonetheless, our result suggests that the C subunit binds the A subunit of PP2A with a binding affinity that is at least an order of magnitude greater than B′ or ST.

This study, together with recent structural and biochemical investigation[27–29], allows us to construct a molecular and quantitative model showing how ST may interfere with the normal functions of PP2A (**Fig. 7b**). In the absence of ST, cellular PP2A exists in two distinct forms: a core enzyme of A-C heterodimer and holoenzymes involving a number of variable regulatory subunits[4]. It is reasonable to assume that the PP2A core enzyme and the PP2A holoenzyme, each with a distinct substrate specificity and phosphatase activity, are in equilibrium in cells. The presence of ST may modify PP2A substrate specificity and phosphatase activity by at least two different modes (**Fig. 7b**). In the first mode, binding of ST to the PP2A core enzyme leads to the formation of a heterotrimeric PP2A–ST complex, which results in inhibition of the phosphatase activity of the PP2A core enzyme. In the second mode, binding of ST to the PP2A core enzyme may shift the equilibrium from the holoenzyme toward the core enzyme, leading to additional changes of substrate specificity and phosphatase activity. Owing to the greater binding affinity of the PP2A core enzyme for the regulatory B′ subunit than for ST, we further speculate that the primary mode of PP2A regulation by ST is through changes in substrate specificity and phosphatase activity as a direct result of binding to the PP2A core enzyme.

Can ST directly displace the regulatory B′ subunit from PP2A holoenzymes? Our *in vitro* studies suggest it can, but perhaps only inefficiently. The key determinants of ST's action in intact cells are the protein expression levels of ST, PP2A core enzyme and the various regulatory subunits. Because ST and the regulatory subunits interact with PP2A core enzyme in a mutually exclusive manner, particular steady-state levels of each of the complexes will be reached, depending upon the concentrations of ST and the regulatory subunits and their K_d values. Overexpression of ST, or of any of the regulatory subunits, would be expected to perturb this equilibrium.

In this study, we also provide evidence that ST may competitively inhibit PP2A phosphatase activity (**Fig. 5d**). This data, in conjunction with binding-affinity measurements (**Fig. 1b** and **Fig. 4c**), indicate that ST may directly interact with the substrate-binding region of the C subunit of PP2A. Our biochemical data further suggest that the J domain may directly mediate this function. In the various PP2A phosphatase assays, ST showed different IC_{50} values, and one explanation for such differences may be the different sizes of the substrates. It is important to note that the differences in IC_{50} values might also be explained by the different substrate concentrations used (0.5 μM for phosphorylase a, 200 μM for the pThr peptide and 10 mM for pNPP), because a higher concentration of substrate will give rise to a higher IC_{50} value. Supporting this notion, IC_{50} was 0.2 μM in the phosphorylase a assay, 2 μM in the pThr peptide assay and not measurable (>10 μM) in the pNPP assay.

ST-mediated regulation of PP2A is likely to be a general feature of other types of PP2A holoenzymes. It is possible that ST preferentially disassembles some PP2A holoenzymes involving specific regulatory subunits, and this process might be modulated by a large number of other proteins that interact with PP2A. Finally, because the regulatory subunits are implicated in cellular localization of PP2A holoenzymes, ST-mediated disassembly of the PP2A holoenzymes may also cause a change in the subcellular distribution of PP2A.

In a broader context, the regulation of PP2A by virtually every interacting protein is probably effected by changes in phosphatase activity and substrate specificity. This applies to the four classes of variable regulatory subunits, as binding of the PP2A core enzyme by a regulatory subunit invariably results in a change of substrate specificity and phosphatase activity. PTPA provides another noteworthy example: it selectively enhances the pTyr phosphatase activity and inhibits the pSer-pThr phosphatase activity[1,41]. Whereas there are 518 kinases in the human genome[42], there are only a handful of serine/threonine phosphatases, creating an apparent conundrum as to how the limited number of phosphatases may cope with the specific actions of many more kinases. The combinatorial approach of regulating substrate specificity of PP2A by a variety of interacting proteins provides a plausible solution to this problem.

METHOD

Protein preparation. All constructs and point mutations were generated using a standard PCR-based cloning strategy. The human A (residues 9–591; α isoform) and C (residues 1–309; α isoform) subunits of PP2A and the regulatory subunits were expressed and purified as described[27,28]. Full-length SV40 ST (1–174) was cloned into pGEX-2T vector (Amersham) and overexpressed at room temperature in *E. coli* strain BL21(DE3) as an N-terminally glutathione *S*-transferase (GST)-tagged protein. The soluble fraction of the *E. coli* cell lysate was first purified using a glutathione (Qiagen) affinity column, then cleaved on the column by thrombin and further purified by ion-exchange (Source 15Q, Amersham) and size-exclusion (Superdex 200, Amersham) chromatography. Purified full-length ST was digested by elastase, which gave rise to a stable core domain of ST. N-terminal peptide sequencing and mass spectroscopy revealed that the core domain contains residues 87–174. The core domain was used to form a stable complex with the A subunit of PP2A or the PP2A core enzyme. The α isoform of the B subunit was expressed in insect cells and purified as a His_6-tagged protein. Purified Bα was incubated with the PP2A core enzyme to form a holoenzyme. The holoenzyme involving the B″ subunit (residues 165–529) was assembled as described[27].

Table 1 Data collection and refinement statistics

	ST bound to A subunit
Data collection	
Space group	$C222_1$
Cell dimensions	
a, *b*, *c* (Å)	137.70, 147.79, 209.65
Resolution (Å)	100.0–3.3 (3.42–3.3)
R_{sym}	0.104 (0.444)
$I / \sigma I$	11.2 (3.6)
Completeness (%)	95.2 (95.6)
Redundancy	8.5 (8.3)
Refinement	
Resolution (Å)	100.0–3.3
No. reflections	30,881
R_{work} / R_{free}	0.249 / 0.313
No. atoms	
Protein	10,358
Ions	4
B-factors	
Protein	72.2
Ions	42.7
R.m.s. deviations	
Bond lengths (Å)	0.010
Bond angles (°)	1.50

X-ray diffraction data were collected on one crystal. Values in parentheses are for highest-resolution shell.

Crystallization and data collection. Crystals of the complex between the A subunit and the core domain of ST were grown by hanging drop vapor diffusion, by mixing the protein ($\sim$10 mg ml^{-1}) with an equal volume of reservoir solution containing 0.2 M $MgCl_2$, 4.5% PEG 1,0000 (w/v) and 0.1 M HEPES (pH 7.5). Crystals appeared overnight and grew to full size within 3–5 d. The crystals belong to space group $C222_1$, with $a = 137.70$ Å, $b = 147.79$ Å and $c = 209.65$ Å. There are two complexes per asymmetric unit. Crystals were equilibrated in a cryoprotectant buffer containing reservoir buffer plus 25% (v/v) glycerol and were flash-frozen in a cold nitrogen stream at –170 °C. The native set was collected at National Synchrotron Light Source beamline X-29 and processed using DENZO and SCALEPACK[43].

Structure determination. The structure of human PP2A–ST complex was determined using PHASER[44] with the atomic coordinates of the PP2A A subunit from the PP2A holoenzyme (PDB 2NPP). The structure of ST was built into model-phased two-fold–averaged $2F_o - F_c$ and $F_o - F_c$ electron density maps. The model was built using O[33] and refined using CNS[45]. There are two molecules of PP2A–ST in each asymmetric unit. Noncrystallographic symmetry restraints were used throughout the refinement. The final refined atomic model contains amino acid residues 9–588 of the PP2A A subunit and residues 91–170 of ST (**Table 1**). Of these residues, 80.8% fall in the most favored region of the Ramachandran plot, and 17.9% and 1.3% are in the additionally and generously allowed regions, respectively.

Phosphatase assays. The phosphatase assays using pNPP and phosphorylase a as substrates were done as described[27]. The phosphatase assay using pTyr peptide (MCA-G-D-A-E-pT-A-A-K(DNP)-R, where MCA is the fluorescence tag (7-methoxycoumarin-4-yl)acetyl and DNP is 2,4-dinitrophenol) was done as described[41]. The concentrations of the PP2A core enzyme were 8 nM (for pNPP and phosphorylase a assays) and 100 nM (for pTyr peptide assay). The concentrations of the substrates were 10 mM (pNPP), 0.5 μM (phosphorylase a)

and 1 μM (pTyr peptide). Ser/Thr Phosphatase Assay Kit 1 (Upstate Biotechnology) was used to measure pThr phosphatase activity according to the manufacturer's protocol. Twenty microliters of each PP2A sample (containing 40 nM PP2A A-C dimer with or without ST) was added to 5 μl phosphopeptide substrate (K-R-pT-I-R-R, 200 μM final concentration). The reaction was done at room temperature for 5 min and stopped by the addition of 100 μl malachite green solution. The samples were kept at room temperature for 10 min to allow color development, and then the absorbance at 650 nm was measured. PP2A alone was used as a blank.

Nondenaturing polyacrylamide gel electrophoresis. All assays were done as described[41].

Isothermal titration calorimetry. ITC was done as described[28]. To obtain a direct binding affinity, 10–20 μM PP2A core enzyme or the A subunit was titrated with 100–200 μM full-length ST, the ST core domain or the C subunit of PP2A, using a VP-ITC microcalorimeter (MicroCal). All proteins were prepared in a buffer containing 25 mM HEPES (pH 8.0) and 150 mM NaCl. The data were fitted by Origin 7.0.

Accession codes. Protein Data Bank: Coordinates have been deposited with accession code 2PKG.

ACKNOWLEDGMENTS

We thank T. Roberts at Harvard Medical School for the complementary DNA encoding SV40 ST, and A. Saxena at the beamlines of the National Synchrotron Light Source, Brookhaven National Laboratory for help. This work was supported by grant R01-CA123155 from the US National Institutes of Health (Y.S.).

AUTHOR CONTRIBUTIONS

Y.C. and Y. Xu designed, performed and analyzed most of the experiments. Q.B. contributed to PP2A enzymology. Y. Xing, Z. Li and Z. Lin provided technical assistance. J.B.S. contributed to discussions. P.D.J. refined the structure. Y.S. led the team and wrote the paper.

COMPETING INTERESTS STATEMENT

The authors declare no competing financial interests.

Published online at http://www.nature.com/nsmb/
Reprints and permissions information is available online at http://npg.nature.com/reprintsandpermissions

1. Janssens, V. & Goris, J. Protein phosphatase 2A: a highly regulated family of serine/threonine phosphatases implicated in cell growth and signalling. *Biochem. J.* **353**, 417–439 (2001).
2. Virshup, D.M. Protein phosphatase 2A: a panoply of enzymes. *Curr. Opin. Cell Biol.* **12**, 180–185 (2000).
3. Lechward, K., Awotunde, O.S., Swiatek, W. & Muszynska, G. Protein phosphatase 2A: variety of forms and diversity of functions. *Acta Biochim. Pol.* **48**, 921–933 (2001).
4. Kremmer, E., Ohst, K., Kiefer, J., Brewis, N. & Walter, G. Separation of PP2A core enzyme and holoenzyme with monoclonal antibodies against the regulatory A subunit: abundant expression of both forms in cells. *Mol. Cell. Biol.* **17**, 1692–1701 (1997).
5. Hemmings, B.A. *et al.* alpha- and beta-forms of the 65-kDa subunit of protein phosphatase 2A have a similar 39 amino acid repeating structure. *Biochemistry* **29**, 3166–3173 (1990).
6. Stone, S.R., Hofsteenge, J. & Hemmings, B.A. Molecular cloning of cDNAs encoding two isoforms of the catalytic subunit of protein phosphatase 2A. *Biochemistry* **26**, 7215–7220 (1987).
7. Green, D.D., Yang, S.I. & Mumby, M.C. Molecular cloning and sequence analysis of the catalytic subunit of bovine type 2A protein phosphatase. *Proc. Natl. Acad. Sci. USA* **84**, 4880–4884 (1987).
8. Arino, J., Woon, C.W., Brautigan, D.L., Miller, T.B., Jr. & Johnson, G.L. Human liver phosphatase 2A: cDNA and amino acid sequence of two catalytic subunit isotypes. *Proc. Natl. Acad. Sci. USA* **85**, 4252–4256 (1988).
9. Moreno, C.S. *et al.* WD40 repeat proteins striatin and S/G(2) nuclear autoantigen are members of a novel family of calmodulin-binding proteins that associate with protein phosphatase 2A. *J. Biol. Chem.* **275**, 5257–5263 (2000).
10. Walter, G. & Mumby, M. Protein serine/threonine phosphatases and cell transformation. *Biochim. Biophys. Acta* **1155**, 207–226 (1993).
11. Janssens, V., Goris, J. & Van Hoof, C. PP2A: the expected tumor suppressor. *Curr. Opin. Genet. Dev.* **15**, 34–41 (2005).
12. Pallas, D.C. *et al.* Polyoma small and middle T antigens and SV40 small t antigen form stable complexes with protein phosphatase 2A. *Cell* **60**, 167–176 (1990).
13. Walter, G., Ruediger, R., Slaughter, C. & Mumby, M. Association of protein phosphatase 2A with polyoma virus medium tumor antigen. *Proc. Natl. Acad. Sci. USA* **87**, 2521–2525 (1990).
14. Sontag, E. *et al.* The interaction of SV40 small tumor antigen with protein phosphatase 2A stimulates the map kinase pathway and induces cell proliferation. *Cell* **75**, 887–897 (1993).
15. Hahn, W.C. *et al.* Enumeration of the simian virus 40 early region elements necessary for human cell transformation. *Mol. Cell. Biol.* **22**, 2111–2123 (2002).
16. Ruediger, R. *et al.* Identification of binding sites on the regulatory A subunit of protein phosphatase 2A for the catalytic C subunit and for tumor antigens of simian virus 40 and polyomavirus. *Mol. Cell. Biol.* **12**, 4872–4882 (1992).
17. Ruediger, R., Hentz, M., Fait, J., Mumby, M. & Walter, G. Molecular model of the A subunit of protein phosphatase 2A: interaction with other subunits and tumor antigens. *J. Virol.* **68**, 123–129 (1994).
18. Ruediger, R., Fields, K. & Walter, G. Binding specificity of protein phosphatase 2A core enzyme for regulatory B subunits and T antigens. *J. Virol.* **73**, 839–842 (1999).
19. Mateer, S.C., Fedorov, S.A. & Mumby, M.C. Identification of structural elements involved in the interaction of simian virus 40 small tumor antigen with protein phosphatase 2A. *J. Biol. Chem.* **273**, 35339–35346 (1998).
20. Scheidtmann, K.H., Mumby, M.C., Rundell, K. & Walter, G. Dephosphorylation of simian virus 40 large-T antigen and p53 protein by protein phosphatase 2A: inhibition by small-t antigen. *Mol. Cell. Biol.* **11**, 1996–2003 (1991).
21. Yang, S.I. *et al.* Control of protein phosphatase 2A by simian virus 40 small-t antigen. *Mol. Cell. Biol.* **11**, 1988–1995 (1991).
22. Kamibayashi, C. *et al.* Comparison of heterotrimeric protein phosphatase 2A containing different B subunits. *J. Biol. Chem.* **269**, 20139–20148 (1994).
23. Cayla, X., Ballmer-Hofer, K., Merlevede, W. & Goris, J. Phosphatase 2A associated with polyomavirus small-T or middle-T antigen is an okadaic acid-sensitive tyrosyl phosphatase. *Eur. J. Biochem.* **214**, 281–286 (1993).
24. Van Hoof, C. & Goris, J. PP2A fulfills its promises as tumor suppressor: which subunits are important? *Cancer Cell* **5**, 105–106 (2004).
25. Pallas, D.C. *et al.* The third subunit of protein phosphatase 2A (PP2A), a 55-kilodalton protein which is apparently substituted for by T antigens in complexes with the 36- and 63-kilodalton PP2A subunits, bears little resemblance to T antigens. *J. Virol.* **66**, 886–893 (1992).
26. Chen, W. *et al.* Identification of specific PP2A complexes involved in human cell transformation. *Cancer Cell* **5**, 127–136 (2004).
27. Xing, Y. *et al.* Structure of protein phosphatase 2A core enzyme bound to tumor-inducing toxins. *Cell* **127**, 341–352 (2006).
28. Xu, Y. *et al.* Structure of the protein phosphatase 2A holoenzyme. *Cell* **127**, 1239–1251 (2006).
29. Cho, U.S. & Xu, W. Crystal structure of a protein phosphatase 2A heterotrimeric holoenzyme. *Nature* **445**, 53–57 (2006).
30. Groves, M.R., Hanlon, N., Turowski, P., Hemmings, B.A. & Barford, D. The structure of the protein phosphatase 2A PR65/A subunit reveals the conformation of its 15 tandemly repeated HEAT motifs. *Cell* **96**, 99–110 (1999).
31. Turk, B., Porras, A., Mumby, M.C. & Rundell, K. Simian virus 40 small-t antigen binds two zinc ions. *J. Virol.* **67**, 3671–3673 (1993).
32. Holm, L. & Sander, C. Protein structure comparison by alignment of distance matrices. *J. Mol. Biol.* **233**, 123–138 (1993).
33. Jones, T.A., Zou, J.-Y., Cowan, S.W. & Kjeldgaard, M. Improved methods for building protein models in electron density maps and the location of errors in these models. *Acta Crystallogr. A* **47**, 110–119 (1991).
34. Mungre, S. *et al.* Mutations which affect the inhibition of protein phosphatase 2A by simian virus 40 small-t antigen in vitro decrease viral transformation. *J. Virol.* **68**, 1675–1681 (1994).
35. Campbell, K.S., Auger, K.R., Hemmings, B.A., Roberts, T.M. & Pallas, D.C. Identification of regions in polyomavirus middle T and small t antigens important for association with protein phosphatase 2A. *J. Virol.* **69**, 3721–3728 (1995).
36. Kim, H.Y., Ahn, B.Y. & Cho, Y. Structural basis for the inactivation of retinoblastoma tumor suppressor by SV40 large T antigen. *EMBO J.* **20**, 295–304 (2001).
37. Cayla, X. *et al.* Isolation and characterization of a tyrosyl phosphatase activator from rabbit skeletal muscle and *Xenopus laevis* oocytes. *Biochemistry* **29**, 658–667 (1990).
38. Van Hoof, C., Cayla, X., Bosch, M., Merlevede, W. & Goris, J. The phosphotyrosyl phosphatase activator of protein phosphatase 2A. A novel purification method, immunological and enzymic characterization. *Eur. J. Biochem.* **226**, 899–907 (1994).
39. Srinivasan, A. *et al.* The amino-terminal transforming region of simian virus 40 large T and small t antigens functions as a J domain. *Mol. Cell. Biol.* **17**, 4761–4773 (1997).
40. Kamibayashi, C., Lickteig, R.L., Estes, R., Walter, G. & Mumby, M.C. Expression of the A subunit of protein phosphatase 2A and characterization of its interactions with the catalytic and regulatory subunits. *J. Biol. Chem.* **267**, 21864–21872 (1992).
41. Chao, Y. *et al.* Structure and mechanism of the phosphotyrosyl phosphatase activator. *Mol. Cell* **23**, 535–546 (2006).
42. Johnson, S.A. & Hunter, T. Kinomics: methods for deciphering the kinome. *Nat. Methods* **2**, 17–25 (2005).
43. Otwinowski, Z. & Minor, W. Processing of X-ray diffraction data collected in oscillation mode. *Methods Enzymol.* **276**, 307–326 (1997).
44. McCoy, A.J., Grosse-Kunstleve, R.W., Storoni, L.C. & Read, R.J. Likelihood-enhanced fast translation functions. *Acta Crystallogr. D. Biol. Crystallogr.* **61**, 458–464 (2005).
45. Brunger, A.T. *et al.* Crystallography and NMR system: a new software suite for macromolecular structure determination. *Acta Crystallogr. D Biol. Crystallogr.* **54**, 905–921 (1998).
46. Kraulis, P.J. Molscript: a program to produce both detailed and schematic plots of protein structures. *J. Appl. Cryst.* **24**, 946–950 (1991).